THE JOURNAL OF BIOLOGICAL CHEMISTRY VOL. 288, NO. 6, pp. 3858–3870, February 8, 2013

Role of Src Homology Domain Binding in Signaling Complexes Assembled by the Murid γ-Herpesvirus M2 Protein*[S]

Received for publication, November 27, 2012, and in revised form, December 20, 2012 Published, JBC Papers in Press, December 20, 2012, DOI 10.1074/jbc.M112.439810

Marta Pires de Miranda[‡§1,2], **Filipa B. Lopes**[‡§1,2], **Colin E. McVey**[¶3], **Xosé R. Bustelo**[‖], **and J. Pedro Simas**[‡§4]

From the [‡]*Instituto de Medicina Molecular and the* [§]*Instituto de Microbiologia, Faculdade de Medicina, Universidade de Lisboa, 1649-028 Lisboa, Portugal, the* [¶]*Instituto de Tecnologia Química e Biológica, Universidade Nova de Lisboa, 2781-901 Oeiras, Portugal, and the* [‖]*Centro de Investigación del Cáncer and Instituto de Biología Molecular y Celular del Cáncer, University of Salamanca, E-37007 Salamanca, Spain*

Background: The M2 γ-herpesvirus protein exploits B cell signaling pathways to promote viral latency.
Results: M2 binds several SH2- and SH3-containing signaling proteins using phosphotyrosine motifs and a proline-rich region, respectively.
Conclusion: These interactions affect the juxtamembranar localization of M2 as well as downstream signaling events.
Significance: M2 may be used as a model to understand modulation of B cells by γ-herpesvirus infection.

γ-Herpesviruses express proteins that modulate B lymphocyte signaling to achieve persistent latent infections. One such protein is the M2 latency-associated protein encoded by the murid herpesvirus-4. M2 has two closely spaced tyrosine residues, Tyr^{120} and Tyr^{129}, which are phosphorylated by Src family tyrosine kinases. Here we used mass spectrometry to identify the binding partners of tyrosine-phosphorylated M2. Each M2 phosphomotif is shown to bind directly and selectively to SH2-containing signaling molecules. Specifically, Src family kinases, NCK1 and Vav1, bound to the Tyr(P)^{120} site, PLCγ2 and the SHP2 phosphatase bound to the Tyr(P)^{129} motif, and the p85α subunit of PI3K associated with either motif. Consistent with these data, we show that M2 coordinates the formation of multiprotein complexes with these proteins. The effect of those interactions is functionally bivalent, because it can result in either the phosphorylation of a subset of binding proteins (Vav1 and PLCγ2) or in the inactivation of downstream targets (AKT). Finally, we show that translocation to the plasma membrane and subsequent M2 tyrosine phosphorylation relies on the integrity of a C-terminal proline-rich SH3 binding region of M2 and its interaction with Src family kinases. Unlike other γ-herpesviruses, that encode transmembrane proteins that mimic the activation of ITAMs, murid herpesvirus-4 perturbs B cell signaling using a cytoplasmic/membrane shuttling factor that nucleates the assembly of signaling complexes using a bilayered mechanism of phosphotyrosine and proline-rich anchoring motifs.

The MuHV-4[5] and its human γ-herpesvirus counterparts, the EBV and Kaposi sarcoma-associated herpesvirus, establish persistent latent infections in memory B cells. To access the memory B cell compartment, these viruses encode proteins that interfere with B cell signaling pathways leading to activation, differentiation, and survival (1). Some of these proteins are thought to drive the proliferation of latently infected B cells in germinal center reactions, which are the site of activation and differentiation of B cells following B cell receptor stimulation by antigen. By driving germinal center reactions, γ-herpesvirus amplify infection and gain physiological access to memory B cells to achieve effective host colonization.

Binding of antigen to the BCR leads to the phosphorylation of ITAMs located in the cytoplasmic tails of the BCR complex. This is carried out by Src family kinases Lyn, Fyn, and BLK and generates phospho-ITAMs that recruit the Syk tyrosine kinase. Phosphorylation cascades triggered by the kinases lead to the assembly of a complex containing adaptor proteins and enzymes, such as Vav1, PLCγ2, and PI3K (2). Signals emanating from this signalosome lead to B cell activation.

Examples of γ-herpesvirus proteins that either mimic or interfere with BCR signaling are the LMP1 and LMP2A encoded by the EBV and K1 and K15 encoded by the Kaposi sarcoma-associated herpesvirus (1). These transmembrane molecules harbor in their cytoplasmic tails protein interaction motifs that mediate the assembly of specific signalosomes. For example, the K1 cytoplasmic domain contains a constitutively

* This work was supported by Portuguese Fundação para a Ciência e Tecnologia (FCT) Grant PTDC/SAU-MII/099314/2008 (to J. P. S.) and Spanish Association Against Cancer and Spanish Ministry of Economy and Competitiveness Grants SAF2009-07172 and RD06/0020/0001, respectively (to X. R. B.). Spanish funding is co-sponsored by the European FEDER program. The SPR equipment at the Instituto de Tecnologia Química e Biológica was acquired with FCT Grant PNRC/692/BIO/2264/2005. The Proteomics Laboratory at the Centro de Investigación del Cáncer is a member of ProteoRed-ISCIII.
[S] This article contains supplemental Figs. S1–S3.
[1] Both authors contributed equally to this work.
[2] Recipient of an FCT fellowship.
[3] Holder of a Ciência 2008 position from the Portuguese Ministry of Science.
[4] To whom correspondence should be addressed. E-mail: psimas@fm.ul.pt.

[5] The abbreviations used are: MuHV-4, murid herpesvirus-4; SH2 and SH3, Src homology 2 and 3, respectively; ITAM, immunoreceptor tyrosine activation motif; BCR, B cell receptor; LMP, latent membrane protein; PLCγ2, phospholipase Cγ2; PRR, proline-rich region; mLANA, mouse latency-associated nuclear antigen; SPR, surface plasmon resonance; eGFP, enhanced green fluorescent protein; PH, pleckstrin homology; aa, amino acids; RU, response units; TRITC, tetramethylrhodamine isothiocyanate.

phosphorylated ITAM that recruits the SH2-containing proteins Lyn, Syk, p85α, PLCγ2, and Vav1, thus promoting the engagement of signaling cascades similar to those triggered upon BCR stimulation (3).

The MuHV-4 does not encode proteins with sequence similarity to such transmembrane proteins (4). By contrast, the unique latency-associated M2 protein from MuHV-4 has been identified as an adaptor protein that modulates B cell signaling and is potentially a functional homologue of the aforementioned viral proteins (5, 6). M2 expression drives B cell proliferation *in vitro* (7), and in a mouse model of infection, M2 is required for the entry of latently infected B cells into germinal center reactions (5, 8–10).

M2 is a 192-amino acid-long proline-rich protein localizing to the nucleus and juxtamembranar areas of the cell (6, 9, 11). M2 binds the SH3 domains of several cellular proteins (6). A C-terminal PRR (residues 153–171) (Fig. 1*A*) containing a consensus class I SH3 binding motif, binds directly to the C-terminal SH3 domain of Vav1 and modulates association of M2 with Vav1 and Fyn in cells (6). In addition, M2 contains two motifs encompassing Tyr^{120} and Tyr^{129} that are differentially and constitutively phosphorylated by Src family kinases (5, 6). The C-terminal SH3-binding PRR is required for phosphorylation of M2, but the mechanism underlying this requirement is unknown. Efficient entry of MuHV-4-infected B cells in germinal center reactions depends on the C-terminal PRR and phosphomotifs present in M2 (5, 12).

The sequence encompassing Tyr^{120} and Tyr^{129} does not form a consensus ITAM (Fig. 1*A*). The $Tyr(P)^{120}$ motif binds the SH2 domains of Vav1 and Fyn (5). This phosphomotif and the C-terminal PRR mediate assembly of a M2-Fyn-Vav1 complex that results in the phosphorylation of Vav1 by Fyn and its catalytic activation (5, 6). M2 expression in B cells drives tyrosine phosphorylation of other proteins in the molecular mass range of 50 to 150 kDa, suggesting that M2 may assemble a larger signalosome (5). Given the relative promiscuity in Tyr(P)-SH2 domain interactions, the $Tyr(P)^{120}$ motif and the so far uncharacterized $Tyr(P)^{129}$ motif could be targeting other SH2 domains.

In this study, we identify new partners of tyrosine-phosphorylated M2 and show that both phosphomotifs are functional, independent SH2 binding sites with different specificities for B cell signaling molecules. M2 is also shown to have an effect in two of the newly identified cellular targets. Specifically, M2 expression drove tyrosine phosphorylation of PLCγ2 and inhibited AKT activation upon BCR stimulation. Finally, the role of the C-terminal PRR of M2 was further investigated. We show that this region of M2 binds strongly to the SH3 domains of Lyn and Fyn and directs M2 to juxtamembranar areas of B cells.

EXPERIMENTAL PROCEDURES

Plasmids—pCMV-myc plasmids encoding wild type M2, M2Y, Y120F, Y129F, and M2P2 proteins have been described (5, 6). To express proteins with an N-terminal enhanced GFP (eGFP), DNA encoding wild type and mutant M2 proteins was cloned into pEGFP-C plasmids (Clontech). The cDNA encoding the PH domain of AKT was subcloned from GFP-PH-AKT (a gift from Dr T. Meyer (Stanford University)) into pmCherry-C1 (Clontech). The cDNA encoding full-length PLCγ2 (pMT2-PLCγ2; a gift from Dr. M. Katan (Institute of Cancer Research, London)) was cloned into pCMV-HA (Clontech). Tyrosine to phenylalanine mutations in PLCγ2 were generated with the QuikChange multisite-directed mutagenesis kit (Stratagene). pGEX Fyn SH2 (aa 145–247) and pGEX Vav1 SH2 (aa 655–774) have been described (5, 13). The DNA sequence encoding the SH2 domains of Lyn (aa 128–226) and NCK1 (aa 281–377) and the N- and C-terminal SH2 domains (termed SH2 N and SH2 C hereafter) of PLCγ2 (SH2 N, aa 532–635; SH2 C, aa 641–674), p85α (SH2 N, aa 332–428; SH2 C, aa 617–724), and SHP2 (tyrosine-protein phosphatase non-receptor 11) (SH2 N, aa 6–102; SH2 C, aa 111–216) was amplified by PCR and cloned into pGEX vectors (GE Healthcare). To express N-terminal His_6-tagged SH3 proteins, the DNA encoding the SH3 domains of PLCγ2 (aa 769–829) and p85α (aa 1–85), the C-terminal SH3 domain of Vav1 (aa 785–842), and the SH3 domain 1 (aa 1–61), 2 (aa 108–165), and 3 (aa 188–252) of NCK1 was cloned into the pQlink H vector (14). DNA encoding the SH3 domains of Fyn (aa 81–144) and Lyn (aa 63–124) and wild type M2 were cloned into pGEX 6P-1. All constructs were confirmed by DNA sequencing.

Pull-down Experiments—For pull-down of cellular proteins with M2 Tyr(P) peptides, 1×10^8 or 2×10^8 cells of the Raji B cell line or 5×10^8 COS1 cells were washed with PBS and lysed with ice-cold lysis buffer (10 mM Tris-HCl, pH 7.4, 100 mM NaCl, 1% Triton X-100, 1 mM $NaVO_4$, 1 mM NaF, and Complete EDTA-free protease inhibitors). Lysates were cleared by centrifugation, and the supernatants were incubated with streptavidin-conjugated Sepharose beads (GE Healthcare) for 4 h at 4 °C. Supernatants were filtered through a 0.45-μm membrane and incubated with 15 μg of pY120 or pY129 (Fig. 1*A*) (5) overnight at 4 °C. Peptide complexes were captured with streptavidin-Sepharose beads. After washing with lysis buffer, proteins were eluted with Laemmli's buffer and resolved on 10% SDS-polyacrylamide gels. Gels were fixed with a 45% methanol, 10% acetic acid solution, for 20 min at room temperature and stained with SYPRO Ruby (Molecular Probes). Individual bands (Fig. 1, *B* and *C*) were excised and processed for MS (15). Binding of SH2 domains to pY120 and pY129 was assessed by pull-down as described (5). Binding of GST-M2 fusion to His-tagged SH3 domains was assessed by GST pull-down assay.

MALDI-TOF MS—Tryptic peptides were analyzed by MALDI-TOF (Ultraflex, Bruker). Identification of protein bands was performed by comparison of the results with the Swiss-Prot database using the MASCOT algorithm (16).

Antibodies—Anti-c-Myc (9E10) was from Clontech. The anti-Tyr(P) (PY99) mAb and anti-PLCγ2 (Q-20), anti-Vav1 (C-14), anti-SH-PTP2 (C-18), anti-Fyn (FYN3), anti-AKT (N-19), and anti-HA (Y-11) polyclonal antibodies were from Santa Cruz Biotechnology, Inc. (Santa Cruz, CA). Anti-GFP and anti-GST polyclonal antibodies were from Abcam and GE Healthcare, respectively. The anti-p85α polyclonal antibody was from Upstate Cell Signaling Solutions. Anti-NCK1 and anti-pS473 AKT mAbs were from BD Transduction Laboratories and Cell Signaling Technology, respectively. Anti-M2, anti-mLANA and anti-pY174 Vav1 rabbit polyclonal antibodies

have been described (6, 17, 18). An anti-mLANA mAb was generated against a GST-mLANA (residues 140–314) fusion protein at the EMBL Monoclonal Antibody Core Facility. Anti-IgG $F(ab')_2$ fragments were from Jackson Immunoresearch. HRP-conjugated Protein A and secondary antibodies were from GE Healthcare and Jackson Immunoresearch.

Tissue Culture and Transfection—S11, A20, and Raji B cells were grown in RPMI 1640 medium supplemented with 10% FBS, 2 mM glutamine, and 100 units/ml penicillin and streptomycin. SYF (19) and COS1 cells were grown in DMEM supplemented as above. A20 B cells were transfected by electroporation as described (5). SYF cells were transfected with FuGENE (Roche Applied Science).

Immunoprecipitation—5×10^7 S11 cells or 2×10^7 A20 B cells transfected with M2 proteins for 24 h were disrupted with ice-cold lysis buffer (10 mM Tris-HCl, pH 7.4, 150 mM NaCl, 1% Triton X-100, 1 mM $NaVO_4$, 1 mM NaF, and Complete EDTA-free protease inhibitors) and processed for immunoprecipitation as described (5). Where indicated, A20 B cells expressing eGFP proteins were isolated using a BD FACSaria flow cytometer (BD Biosciences) prior to lysis.

Proteins—Proteins were expressed in *Escherichia coli* BL21 (DE3) pRARE2. GST fusion proteins were purified with glutathione-Sepharose (GE Healthcare). For SPR experiments, the GST partner was removed by protease cleavage to avoid avidity effects due to dimerization of GST. Cleaved SH domains were further purified and buffer-exchanged into HBS-EP (10 mM Hepes, pH 7.4, 150 mM NaCl, 3 mM EDTA, 0.005% polysorbate 20) by gel filtration using a Superdex 75 10/300 GL column (GE Healthcare). Single peaks corresponding to monomeric SH domains were used in the SPR assays. His_6-tagged proteins were purified on nickel-nitrilotriacetic acid-agarose (Qiagen).

Surface Plasmon Resonance—These experiments were performed with the Biacore 2000 system (GE Healthcare) at 25 °C. Biotinylated pY120 and pY129 (Fig. 1*A*) and a biotinylated peptide comprising the M2 C-terminal PRR (aa 153–171, GPPTRPLPKLPNQHPMNPE; purchased from Sigma), named M2(153–171), were diluted in HBS-EP and immobilized onto streptavidin-coated sensor chip SA (GE Healthcare) to the indicated response units (RU). Serial dilutions of the SH2 and SH3 proteins were prepared in HBS-EP and injected through peptide and control blank cells. Dissociation was in running buffer, and regeneration, if required, was achieved with a pulse injection of HBS-EP with 1 M NaCl. Bound protein was the difference between signal in peptide and in the control cells (supplemental Figs. S1 and S2). The equilibrium dissociation constant, K_D, was determined by non-linear fitting of the data using a 1:1 Langmuir isotherm.

Immunofluorescence—Transfected A20 B cells were added to poly-L-lysine-coated coverslips (BD Biosciences), incubated for 30 min at room temperature, and processed for immunofluorescence. SYF cells were grown on coverslips and transfected for 48 h before fixation. Cells were fixed with 4% paraformaldehyde, PBS for 20 min at room temperature and permeabilized for 10 min in 0.2% Triton X-100, PBS. Samples were stained with primary antibodies for 1 h at room temperature followed by detection with the indicated species-specific Alexa Fluor-conjugated antibodies (Molecular Probes, Invitrogen). Filamentous (F)-actin was stained with TRITC-phalloidin (Sigma), and DNA was detected with DAPI (Invitrogen). PBS washes were performed between all steps. Coverslips were mounted in Mowiol (Fluka). Images were collected with a LSM 510 META Zeiss confocal microscope using LSM 510 software and processed with ImageJ.

RESULTS

Identification of Proteins Interacting with Tyrosine-phosphorylated M2—We have employed a proteomic approach to identify cellular binding partners of tyrosine-phosphorylated M2. Biotinylated peptides encompassing $Tyr(P)^{120}$ or $Tyr(P)^{129}$ (termed pY120 and pY129, respectively; see Fig. 1*A*) (5) were used to pull down proteins from Raji B cell lysates. Peptide complexes were precipitated with streptavidin beads, resolved by SDS-PAGE, and stained with SYPRO Ruby (Fig. 1*B*). Proteins that associated specifically with the peptides but not with beads alone were identified by MS. Vav1 was identified in lane 2 (Fig. 1*B* and Table 1), confirming the interaction with pY120 (5). Similarly, the adaptor protein NCK1 and Lyn were exclusively found in pY120 precipitates (Fig. 1*B*, *lanes 2* and *4*, and Table 1). The association of a Src family kinase with pY120 is not unexpected because we have shown before that Fyn binds to this peptide (5). The PI3K regulatory α subunit (p85α) precipitated in equivalent amounts with both pY120 and pY129 (Fig. 1*B*, *lanes 2–4*, and Table 1). PLCγ2, the tyrosine-protein phosphatase SHP2, and the focal adhesion kinase FAK2 were identified in pY129 precipitates only (Fig. 1*B*, *lane 3*, and Table 1). Tubulin and actin associated with pY120 or both peptides, respectively (Fig. 1*B*, *lanes 3* and *4*, and Table 1), which could be due to a nonspecific association with beads or to the presence of cytoskeleton interacting proteins in the precipitates. Similar pull-down experiments were performed using COS1 cell lysates (Fig. 1*C*). In this case, we identified NCK1, two ubiquitous Src family kinases (Fyn and Yes), and the catalytic subunit of PI3K (PK3CB) in pY120 precipitates, whereas PLCγ1, a non-hematopoietic isoform of PLCγ2, and SHP2 were found in association with pY129 (Fig. 1*C* and Table 1). Vav1 was not detected in these experiments because its expression is restricted to hematopoietic cells (20, 21). All identified proteins, except Vav1 and Src family kinases, are previously unknown targets of M2.

Binding of M2 to SH2 Domains—Apart from FAK2, PK3CB, and the cytoskeleton proteins, proteins found in pY120 and pY129 precipitates contain one or two SH2 domains and, with the sole exception of the SHP2, at least one SH3 domain (Fig. 2*A*). The SH2 domains of Vav1 and Fyn bind $Tyr(P)^{120}$ (5). Therefore, we next assessed if the cellular proteins identified here also bound directly to the M2 phosphomotifs via their SH2 domains. M2 phosphopeptides were used to pull-down individual SH2 domains expressed as GST fusion proteins in bacteria. The GST-SH2 domains of Vav1 and Fyn were included as a comparison. Binding of GST proteins to each peptide was assessed by anti-GST immunoblots. All GST-SH2 proteins, but not the non-chimeric GST, bound with varying strengths to at least one of the phosphopeptides (Fig. 2*B*, *first* and *second panels* from the *top*). The differences in binding were a reflection of distinct selectivity because similar amounts of fusion proteins were used in each pull-down (Fig. 2*B*, *bottom*). To explore fur-

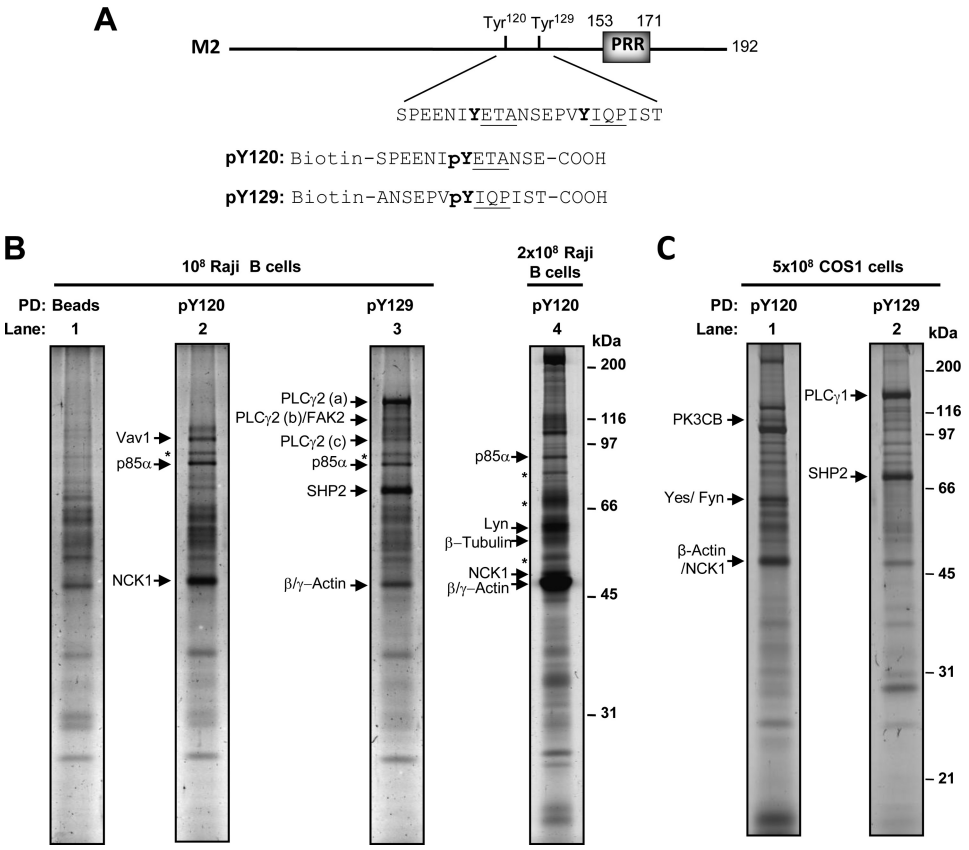

FIGURE 1. *A*, schematic diagram of the M2 protein depicting Tyr^{120} and Tyr^{129} and the position of the C-terminal PRR. The sequence containing Tyr^{120} and Tyr^{129} differs from the consensus ITAM sequence (*YXX*(L/I)X_{6-8}*YXX*(L/I)). Biotinylated phosphotyrosine peptides matching the sequence of M2 between residues 114 and 126 (pY120) or between residues 123 and 135 (pY129) are shown. Tyrosine and Tyr(P) residues are *highlighted* in *boldface type*. Residues at positions +1 to +3 relative to each tyrosine or phosphotyrosine that influence SH2 binding specificity are *underlined*. *B* and *C*, SYPRO Ruby-stained SDS-PAGE reducing gels depicting proteins that interacted with M2 phosphopeptides. Lysates from the indicated cells were incubated with pY120 or pY129. Complexes were recovered with streptavidin-coupled agarose beads, and proteins were resolved by SDS-PAGE and stained with SYPRO Ruby. As a negative control, lysates were also incubated with beads alone (*B*, *lane 1*). Molecular mass markers are depicted on the *right* in kDa. *Arrows* to the *left* of the *lanes* indicate bands identified by MALDI-TOF. *Asterisks* denote bands for which no significant identity was obtained. In *B*, *lane 3*, PLCγ2 was identified in three bands denoted as *a*, *b*, and *c*. See Table 1 for details on identification of the indicated bands. *PD*, pull-down.

TABLE 1

Identification of proteins that interacted with M2 tyrosine-phosphorylated peptides

Bands indicated by *arrows* in Fig. 1, *B* and *C*, were excised from the gels, digested with trypsin, and identified by MALDI-TOF mass spectrometry. MASCOT scores of >54 (Raji B cells) or >59 (COS1 cells) were considered significant ($p < 0.05$).

Cells	Peptide	Lane	Protein	UniProtKB accession number	Theoretical molecular mass	Identified peptides	Coverage	MASCOT score
					kDa		%	
Raji B cells	pY120	2	Vav1	P15498	99	11	13	87
			p85α	P27986	83	11	13	86
			NCK1	P16333	43	18	51	216
	pY129	3	PLCγ2(a)	P16885	149	17	16	126
			PLCγ2(b)/FAK2	P16885/Q14289	149/117	18/16	13/20	110/105
			PLCγ2(c)	P16885	149	14	11	122
			p85α	P27986	83	12	15	108
			SHP2	Q06124	68	22	35	254
			β/γ-Actin	P60709/P63261	42/42	10/10	37/37	122/122
	pY120	4	p85α	P27986	83	17	23	184
			Lyn	P07948	58	15	34	215
			β-Tubulin	P07437	50	7	19	72
			NCK1	P16333	43	14	32	173
			β/γ-Actin	P60709/P63261	42/42	14/14	42/42	229/229
COS1 cells	pY120	1	PK3CB	P42338	124	23	27	243
			Yes/Fyn	P07947/P39688	61/60	24/24	20/13	106/60
			β-Actin/NCK1	P60712/P16333	42/43	13/13	46/38	112/103
	pY129	2	PLCγ1	P19174	149	19	19	177
			SHP2	Q06124	68	16	30	173

ther the global SH2 binding properties of the phosphopeptides, we conducted binding analyses using SPR. The SH2 domains with weaker association in the pull-down assays are likely to contribute less to the interaction of the full-length proteins with the phosphomotifs and were excluded from the analyses (Fig. 2*B*, *top panels*, *lanes 2*, *4*, and *7*). M2 phosphopeptides

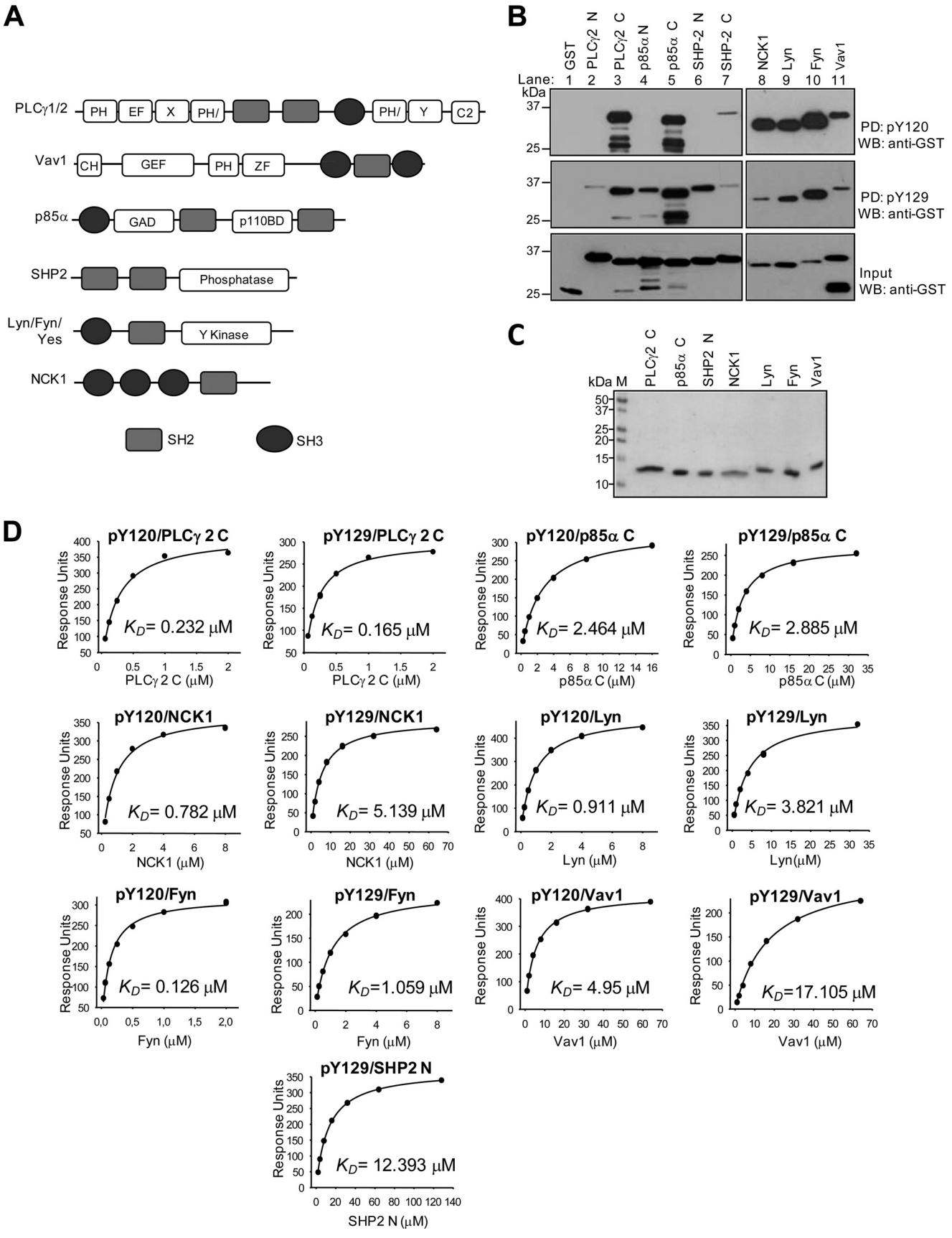

TABLE 2
Affinity of SH2 domains for M2 tyrosine-phosphorylated peptides
ND, not determined; N, N-terminal SH2 domain; C, C-terminal SH2 domain; *n*, number of experiments performed.

SH2 domain	pY120 Mean K_D	pY120 K_D range	pY120 *n*	pY129 Mean K_D	pY129 K_D range	pY129 *n*
	μM	μM		μM	μM	
Fyn	0.118	0.113–0.126	3	1.086	1.059–1.112	2
PLCγ2 C	0.252	0.232–0.273	2	0.179	0.165–0.192	2
Lyn	0.796	0.627–0.911	3	3.821		1
NCK1	0.887	0.782–0.981	4	6.048	5.139–6.555	3
p85α C	2.471	2.464–2.477	2	2.662	2.885–2.438	2
Vav1	5.412	4.950–6.838	4	17.166	15.565–18.829	3
SHP2 N	ND	ND	2	12.279	12.164–12.393	2

were immobilized on a streptavidin chip, and binding to purified SH2 domains (Fig. 2*C*) was probed at a range of concentrations. In parallel, the signal from a control blank channel in the same chip was measured and subtracted from that of each peptide channel to give bound protein. Binding data were characteristic of interactions with rapid kinetics (supplemental Fig. S1) and enabled determination of the K_D value by non-linear fitting of binding values at equilibrium (Fig. 2*D*; listed in Table 2). The SH2 domains of Vav1, NCK1, and Src family kinases Fyn and Lyn bound preferentially to pY120 with strong to moderate affinity (118 nM to ~5 μM) and much more weakly to pY129 (1–17 μM). These results explain why, at lower protein concentrations, such as those in cell extracts, we only detected association of the full-length proteins with pY120 (Fig. 1, *B* and *C*). The C-terminal SH2 domain of p85α bound with equivalent affinity (~2 μM) to both phosphopeptides, and the N-terminal SH2 domain of SHP2 bound weakly (12.279 μM) to Tyr(P)^{129} and nearly undetectably to Tyr(P)^{120} (Fig. 2*D* and supplemental Fig. S1). These results agree with pull-down data (Fig. 1, *B* and *C*). The C-terminal SH2 domain of PLCγ2 bound strongly (179 nM) to pY129 and, surprisingly, with a similar albeit slightly lower affinity to pY120 (252 nM).

M2 Assembles Multiprotein Complexes in B Cells—We next conducted immunoprecipitation experiments to assess if M2 associated with PLCγ2, p85α, SHP2, and NCK1 in B cells and to determine which M2 motifs would be involved in the interactions. Myc-tagged wild type M2 or mutant proteins with Tyr^{120} and/or Tyr^{129} replaced by phenylalanine (Y120F, Y129F, and Y120F/Y129F (M2Y) mutants) were transiently expressed in A20 B cells. We included in our analysis M2P2, an M2 mutant protein that has the C-terminal PRR disrupted and binds poorly to Vav1 (6). PLCγ2, p85α, SHP2, and NCK1 were immunoprecipitated from cellular extracts, and bound M2 proteins were detected by anti-Myc immunoblots. Wild type and Y129F proteins associated in equivalent amounts with all immunoprecipitated proteins (Fig. 3, *A–D*, *top panels*, *lanes 2* and *5*). This association was dramatically reduced in the case of M2Y and M2P2 (Fig. 3, *A–D*, *top panels*, *lanes 3* and *6*). Disruption of Tyr^{120} had no effect on binding of M2 to PLCγ2 but greatly diminished the interaction of the viral protein with the other cellular targets (Fig. 3, *A–D*, *top panels*, *lane 4*).

To determine if M2 formed multiprotein complexes with the proteins identified here, PLCγ2 immunoprecipitates were probed for the presence of the other M2 cellular targets. In the presence of wild type or the Y129F M2 protein, NCK1, Fyn, p85α, and Vav1 co-immunoprecipitated with PLCγ2 (Fig. 3*A*, *top panels*, *lanes 2* and *5*). SHP2 was not detected in these precipitates. In parallel Tyr(P) immunoblots, we assessed the phosphorylation of proteins in all of the above immunoprecipitates. Although phosphorylation of p85α, NCK1, and SHP2 was undetectable in all experimental conditions (data not shown), PLCγ2 was consistently phosphorylated upon expression of wild type M2 (Fig. 3*A*, *top*, *lane 2*). As described before (5), wild type and Y129F M2 proteins and co-immunoprecipitated Vav1 were all tyrosine-phosphorylated (Fig. 3*A*, *second* and *third panels* from *top*, *lanes 2* and *5*). M2 therefore assembles a range of complexes with PLCγ2, p85α, NCK1, Vav1, Src family tyrosine kinases, and SHP2 in B cells. The Tyr(P)^{120} motif is required for the formation of M2 complexes containing Vav1, Fyn, NCK1, and p85α and to drive phosphorylation of Vav1. Either Tyr(P) motif is sufficient to allow association of M2 with PLCγ2, but both motifs are needed to drive phosphorylation of PLCγ2. Pull-down assays using GST-M2 and His-tagged SH3 domains revealed that the SH3 domains of PLCγ2, p85α, and NCK1 do not bind directly to M2 (supplemental Fig. S3). Thus, unlike Vav1, Fyn and Lyn, which bind M2 via SH3 and SH2 domains, direct binding of PLCγ2, p85α, NCK1, and SHP2 to M2 occurs solely via Tyr(P)-SH2 interactions. The decreased interaction of the latter proteins with M2P2 (Fig. 3, *A–D*, *lane 6*) could be due to lower phosphorylation levels of this mutant (5, 6).

Immunoprecipitation experiments in murine B lymphoma S11 cells, which are predominantly infected with latent MuHV-4 (22), revealed that M2 co-immunoprecipitated with PLCγ2 and p85α (Fig. 3, *E* and *F*, *top panels*, *lane 2*). Immunoprecipitation with an unrelated antibody against a key latency-associated viral protein, mLANA, did not yield detectable M2 (Fig. 3, *E* and *F*, *top panels*, *lane 1*). Therefore, in a context of infection and endogenous M2 expression, M2 associates with both of these enzymatic targets.

FIGURE 2. **SH2 domains bind each of the M2 phosphomotifs with different affinities.** *A*, schematic diagram of SH2-containing proteins identified by MS. *Gray rectangles*, SH2 domains; *dark gray ellipses*, SH3 domains. Other represented domains are pleckstrin homology (*PH*), elongation factor-hand (*EF*), phospholipid binding (*C2*), PLCγ2 catalytic domains (*X* and *Y*), bipartite PH (*PH/*), calponin homology (*CH*), guanidine exchange factor (*GEF*) catalytic domain of Vav1, zinc finger (*ZF*), break point homology (*BH*), and p110 binding domain (*p110BD*). *B*, pull-down of GST or GST-SH2 fusion proteins with pY120 (*top*) or pY129 (*middle*). GST fusion proteins were incubated with the biotinylated peptides, and the peptide complexes were captured with streptavidin-Sepharose beads. Precipitated proteins were detected by anti-GST immunoblotting. An aliquot of the purified recombinant proteins was also analyzed by Western blot to demonstrate that similar amounts of each protein were used in the pull-downs (*bottom*). The positions of molecular size markers are indicated to the *left* of the *panels*. *C*, Coomassie Blue-stained SDS-PAGE gel depicting the purified SH2 domains used in the SPR experiments. *M*, molecular weight markers. *D*, binding affinity of SH2 domains for M2 phosphomotifs as determined by SPR. The indicated SH2 domains were injected at 5–10 μl/min for 1–3 min over empty flow cells or cells containing immobilized pY120 (~30 RU) or pY129 (~25 RU). At each concentration, bound protein was the difference between the response at equilibrium between the peptide and empty flow cells. The equilibrium dissociation constant, K_D, was calculated by non-linear fitting of the equilibrium binding data. With the exception of the Lyn SH2-pY129 interaction, data are representative of at least two independent experiments. *PD*, pull-down; *WB*, Western blot; *N*, N-terminal SH2 domain; *C*, C-terminal SH2 domain.

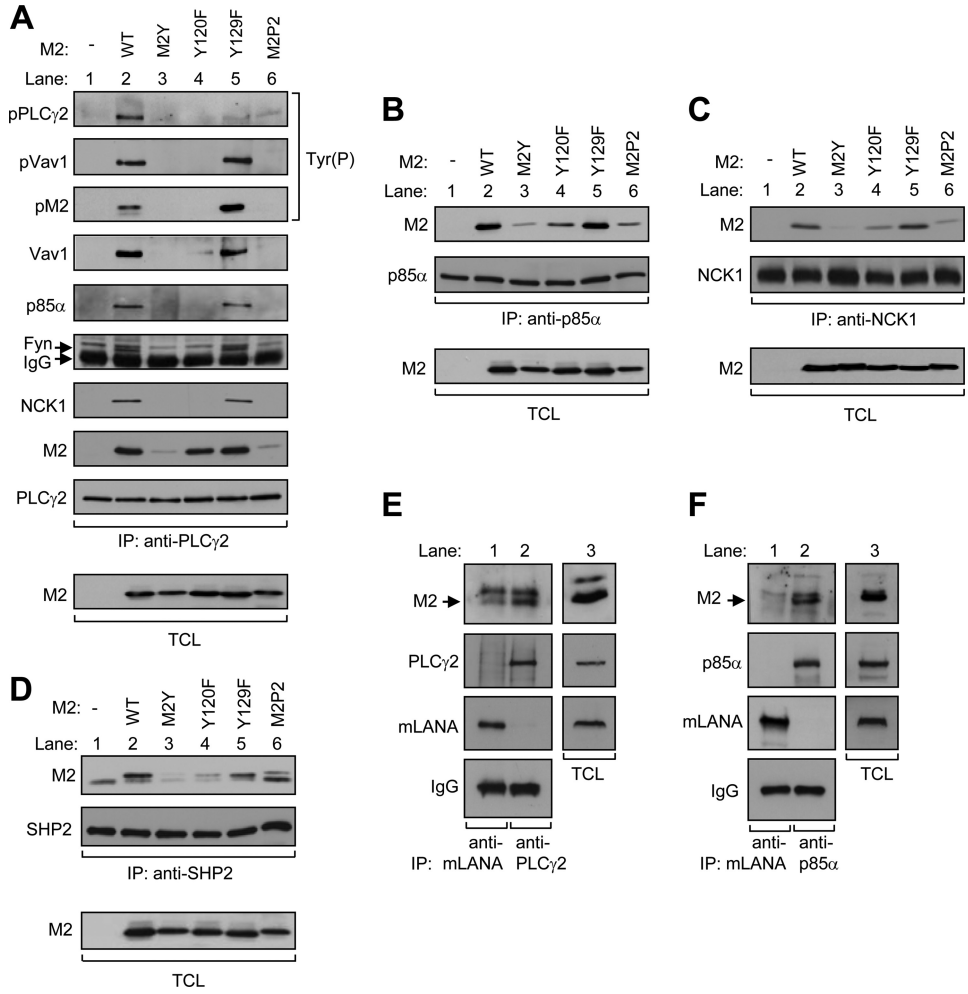

FIGURE 3. **M2 assembles multiple signaling complexes in B cells.** *A–D*, A20 B cells transiently expressing Myc-tagged wild type (*WT*) or the indicated M2 mutant proteins were lysed, and cleared lysates were incubated with anti-PLCγ2 (*A*), anti-p85α (*B*), anti-NCK1 (*C*), or anti-SHP2 (*D*) antibodies. Immunoprecipitates (*top panels*) were analyzed by Western blotting with specific antibodies against Vav1, NCK1, Fyn, p85α, PLCγ2, SHP2, or Tyr(P), and an anti-Myc antibody was used to detect M2 proteins (*top panels*). Anti-Myc immunoblots were performed in an aliquot of the total cellular lysates to confirm ectopic expression of M2 proteins (*bottom panels*). Tyrosine-phosphorylated PLCγ2, Vav1, and M2 are denoted as *pPLCγ2*, *pVav1*, and *pM2*, respectively. *E* and *F*, lysates from S11 cells were precleared with Protein G-Sepharose beads and then incubated with rabbit anti-mLANA or anti-PLCγ2 IgG (*E*) or with rabbit anti-mLANA or anti-p85α sera (*F*). Immunocomplexes, captured with Protein G-Sepharose beads, and an aliquot of the total cellular lysates were resolved by SDS-PAGE and analyzed by Western blotting using anti-PLCγ2 (*E*) or anti-p85α (*F*) polyclonal antibodies and an anti-mLANA mAb. To identify M2, a rabbit polyclonal anti-M2 antibody was used, followed by detection with HRP-conjugated Protein A instead of a secondary antibody, in order to diminish signal derived from light chains of antibodies used in the immunoprecipitation (*top panels*). *Arrows* to the *left* of the *panels* indicate the band corresponding to M2. *IP*, immunoprecipitation; *TCL*, total cellular lysates.

M2 Drives Tyrosine Phosphorylation of PLCγ2 at Activation Sites and Inhibits AKT upon BCR Activation—Upon BCR stimulation, phosphorylation of PLCγ2 occurs at Tyr^{753}, Tyr^{759}, and C-terminal Tyr^{1197} and Tyr^{1217} (23–27). Phosphorylation of Tyr^{753} and Tyr^{759} correlates with PLCγ2 activation (24–26, 28). To identify the sites of M2-driven PLCγ2 phosphorylation, we used a series of tyrosine to phenylalanine mutants targeting these four sites (Fig. 4, *A* and *B*). The HA-tagged mutants or wild type PLCγ2 were expressed alone or together with wild type M2 in A20 B cells. PLCγ2 proteins were immunoprecipitated with an anti-HA mAb, and phosphorylation was assessed by Tyr(P) immunoblots. M2 expression drove robust phosphorylation of transfected wild type PLCγ2 (Fig. 4, *A* and *B*, *top panel*, *lane 4*), confirming results observed with endogenous protein (Fig. 3*A*, *top*, *lane 2*). All PLCγ2 mutants displayed diminished phosphorylation when compared with the wild type protein, indicating that all four sites are phosphorylated upon M2 expression (Fig. 4, *A* and *B*, *top panels*). Notably, this decrease was higher in the PLCγ2 C-terminal mutants, which suggests that Tyr^{1197} and Tyr^{1217} are favored phosphorylation sites. All PLCγ2 proteins were expressed in equivalent amounts (Fig. 4, *A* and *B*, *bottom panels*).

To assess the effect of M2 binding to p85α on PI3K pathways, we investigated the activation status of AKT, a serine/threonine kinase that is a downstream effector of PI3K, upon M2 expression. PI3K activation leads to the production of PIP3 and recruitment of AKT to the plasma membrane via its pleckstrin homology domain (29). Membrane anchorage is required for phosphorylation of AKT on Ser^{473} and its full activation (30). Expression of eGFP-tagged M2 in A20 B cells inhibited translocation of the mCherry-tagged PH-AKT to the plasma membrane upon BCR stimulation (Fig. 5, *A* (*middle panels*) and *B*). This effect was dependent on the phosphorylation of M2, because it was reverted when the eGFP-M2Y mutant protein

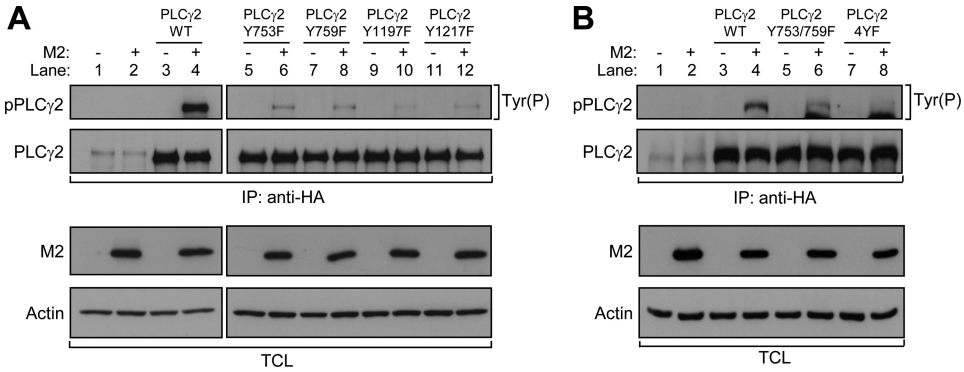

FIGURE 4. **M2 induces tyrosine phosphorylation of PLCγ2 at activation sites.** *A* and *B*, A20 B cells were transfected with plasmids encoding HA-tagged wild type (*WT*) PLCγ2 or tyrosine to phenylalanine mutant versions of PLCγ2, alone or together with pCMV-myc wild type M2. The PLCγ2 4YF protein has compound tyrosine to phenylalanine mutations of Tyr^{753}, Tyr^{759}, Tyr^{1197}, and Tyr^{1217}. Twenty-four hours after transfection, cell extracts were prepared and subjected to immunoprecipitation with a rabbit polyclonal anti-HA antibody. Immunocomplexes were resolved by SDS-PAGE and analyzed by Western blotting with anti-Tyr(P) and anti-PLCγ2 antibodies (*top panels*). Tyrosine-phosphorylated PLCγ2 is denoted as pPLCγ2. An aliquot of the total cellular lysates was also analyzed by Western blot using anti-Myc antibodies to confirm expression of M2 in the appropriate samples (*bottom panels*). Anti-actin immunoblots confirmed that equivalent amount of cellular extracts were used in each experimental condition (*bottom panels*). −, without; +, with; *IP*, immunoprecipitation; *TCL*, total cellular lysates.

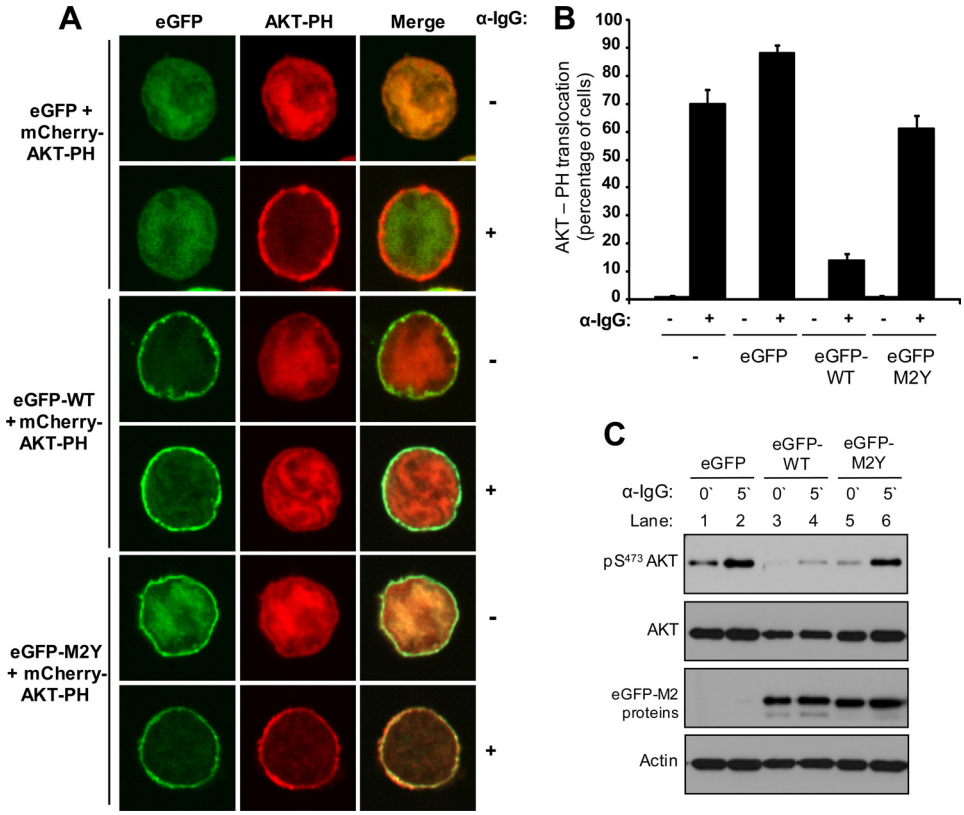

FIGURE 5. **M2 expression inhibits AKT translocation to the plasma membrane and its phosphorylation upon BCR stimulation.** *A*, A20 B cells expressing the mCherry-tagged PH domain of AKT and eGFP (*two top panels*), eGFP-tagged wild type (*WT*) M2 (*two middle panels*), or M2Y (*two bottom panels*) were unstimulated (−) or stimulated (+) with 10 μg/ml anti-IgG F(ab′)2 for 5 min. *B*, quantification of mCherry-PH-AKT translocation to the plasma membrane as observed in *A*. *Bars*, mean percentage of co-transfected cells where PH-AKT localized at the plasma membrane. *Error bars*, S.D. value of three independent experiments. In each experiment, 100 doubly transfected cells/condition were scored. *C*, M2 expression reduces phosphorylation of AKT on Ser^{473}. A20 B cells transiently expressing eGFP-tagged wild type (*WT*) M2 or the M2Y mutant protein were sorted by flow cytometry 24 h after transfection. Cells were unstimulated (−) or stimulated (+) as in *A* and lysed, and an aliquot of the total cellular lysates was analyzed by Western blot analysis using specific antibodies against phospho-Ser^{473} (*pS^{473}*) AKT, AKT, M2, and actin.

was expressed (Fig. 5, *A* (*bottom panels*) and *B*). Consistently, expression of wild type M2, but not the M2Y protein, in A20 B cells prevented phosphorylation of AKT on Ser^{473}, an effect evident after BCR stimulation (Fig. 5*C*, *top*).

Juxtamembrane Localization of M2 Depends on the C-terminal PRR SH3 Binding Motif and Src Family Kinase Expression—M2 localizes to the nucleus and in juxtamembrane actin-rich areas of the cytoplasm in fibroblasts and predominantly near the plasma membrane in B cells (6, 9, 11). To assess if the M2 SH3 and SH2 binding sites had a role in determining its subcellular localization, we examined the distribution of eGFP-tagged M2 proteins in A20 B cells (Fig. 6*A*). All eGFP-M2 proteins expressed in equivalent amounts, and wild type M2 and Y129F proteins drove phosphorylation of Vav1 (Fig. 6*B*). Thus, the

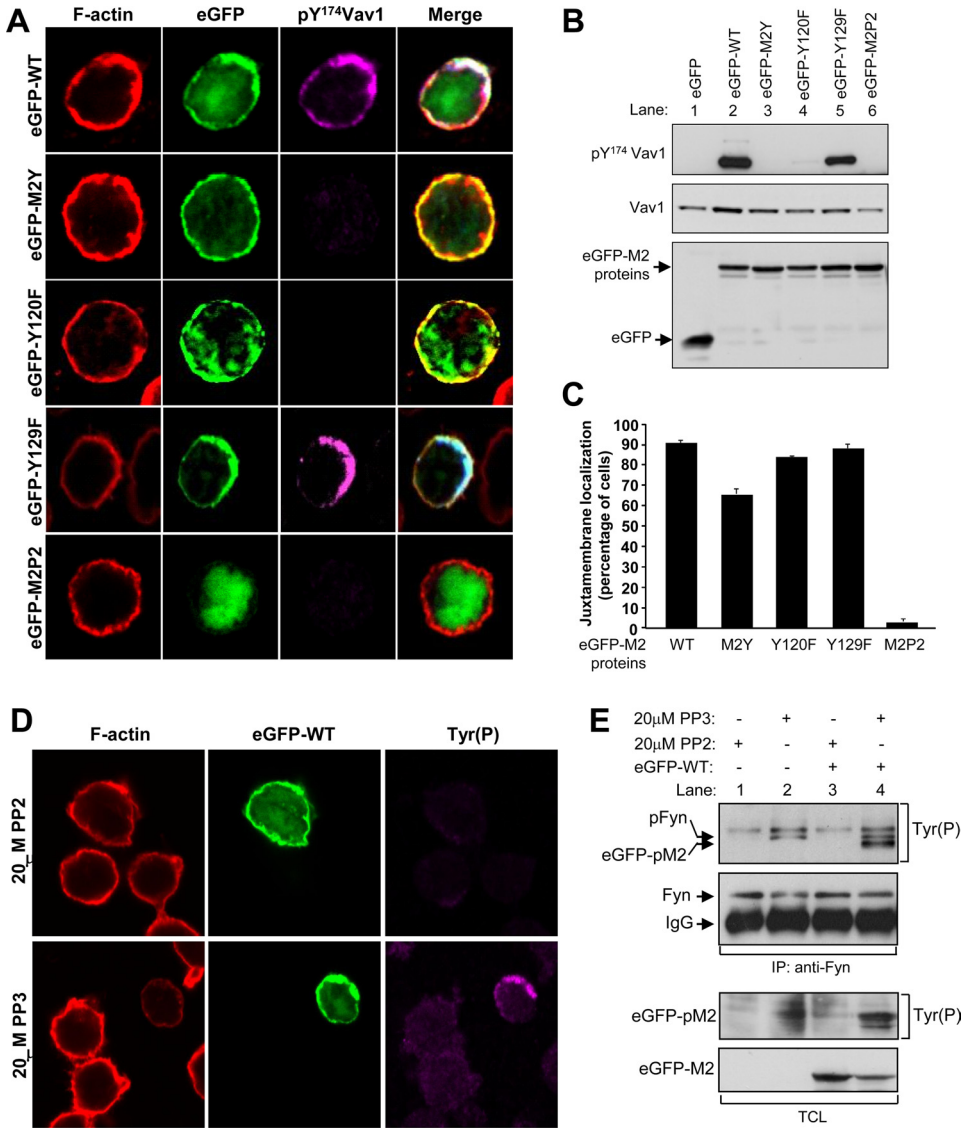

FIGURE 6. **The C-terminal SH3 binding motif of M2 determines juxtamembrane localization in B-cells.** *A*, A20 B cells expressing eGFP-tagged wild type or the indicated M2 mutant proteins. F-actin was stained with TRITC-phalloidin, and active Vav1 was detected with an anti-pY174 Vav1 antibody and an Alexa Fluor 647-conjugated secondary antibody. *B*, Western blot analysis of A20 B cell lysates expressing the indicated proteins. eGFP and eGFP-tagged M2 proteins were detected with an anti-GFP antibody, total Vav1 was detected with anti-Vav1, and active Vav1 was detected with anti-pY174 Vav1. *C*, quantification of cells with juxtamembrane localization of M2 proteins. *Bars*, mean percentage of transfected cells where wild type or M2 mutant proteins localized near the plasma membrane. *Error bars*, S.D. value of three independent experiments. In each experiment, 100 transfected cells/condition were scored for juxtamembrane localization of M2. *D*, localization of eGFP-tagged wild type M2 in A20 B cells incubated for 30 min at 37 °C with 20 μM Src family kinase inhibitor PP2 or its inactive analog, PP3. F-actin was stained with TRITC-phalloidin, and tyrosine phosphorylation was detected with an Alexa Fluor 647-conjugated anti-Tyr(P) antibody. *E*, Western blot analysis of Fyn tyrosine phosphorylation in A20 B cells treated with PP2 and PP3 as in *D*. Mock-transfected cells or cells expressing wild type eGFP-tagged M2 were lysed, and the cleared lysates were subjected to immunoprecipitation with an anti-Fyn antibody, followed by Western blot analysis with an anti-Tyr(P) antibody (*top panel*, *top arrow*). Anti-Fyn immunoblots were performed to confirm equivalent levels of immunoprecipitated Fyn in each condition (*second panel* from *top*). An aliquot of the total cellular lysates was analyzed by Western blot using an anti-Tyr(P) antibody (*third panel* from *top*) and an anti-GFP antibody (*bottom panel*). Tyr(P) bands corresponding to phosphorylated Fyn (*pFyn*) or consistent with the size of eGFP-tagged phosphorylated M2 (pM2) are indicated by *arrows* on the *left side* of the *panels*. −, without; +, with; *IP*, immunoprecipitation; *TCL*, total cellular lysates.

eGFP tag did not interfere with M2 function. Wild type M2 predominantly co-localized with actin near the plasma membrane (~90% of transfected cells; Fig. 6, *A* (*top panels*) and *C*) and to a much lesser extent in the nucleus. The tyrosine mutants had a distribution similar to that of the wild type protein (Fig. 6, *A* (*three middle panels*) and *C*). The M2P2 protein, however, seldom localized near the plasma membrane (less than 5% of transfected cells; Fig. 6*C*) and was mainly found in the nucleus (Fig. 6*A*, *bottom panels*). As expected, both wild type M2 and the Y129F protein co-localized with Vav1 and drove its phosphorylation (Fig. 6, *A* and *B*). PP2, an Src family kinase inhibitor, but not PP3, its inactive homologue, inhibited the phosphorylation of M2 in A20 B cells but had no effect on its subcellular localization (Fig. 6, *D* and *E*). Thus, the juxtamembranar localization of M2 is independent of its phosphorylation status or Src family tyrosine kinase activity. In contrast, the C-terminal PRR is required to concentrate M2 near the plasma membrane, possibly by mediating binding to an SH3-containing protein.

Immunoprecipitation experiments have shown that the M2 C-terminal PRR modulates the interaction of M2 with Fyn (6). However, evidence of direct binding of this region of M2 to the

SH3 domains of Src family kinases is lacking. SPR analyses revealed that a synthetic peptide comprising the C-terminal PRR of M2 bound the purified SH3 domains of Fyn and Lyn, with a higher affinity for the SH3 domain of Lyn (Fig. 7, *A* and *B*). Notably, the affinity values obtained are strikingly close to those observed between the SH3 domains of these kinases and proline-rich peptides derived from the cytoplasmic tails of K15, Tip, and Tio, all transmembrane signaling proteins from simian γ-herpesvirus (31–33). Because active Src family kinases localize in actin-rich membrane ruffles (34), we hypothesized that Fyn or Lyn could be recruiting M2 to the plasma membrane. To address this issue, we investigated the localization of eGFP-tagged M2 proteins in SYF fibroblasts, which lack Src, Yes, and Fyn, the ubiquitously expressed Src kinases (19). Wild type M2, M2Y, and M2P2 localized predominantly in the nucleus of SYF cells (Fig. 7*C*). However, upon co-expression with Fyn, wild type M2 and M2Y localized in the nucleus and in membrane ruffles, whereas the M2P2 protein remained exclusively nuclear (Fig. 7*D*). Thus, Src family kinases are required for the juxtamembrane localization of M2 possibly by directly recruiting the viral protein.

DISCUSSION

In this work, we have expanded the set of binding partners of phosphorylated M2 and show that, in addition to the $Tyr(P)^{120}$ motif, the motif encompassing $Tyr(P)^{129}$ also targets SH2 domains. By screening the cellular proteins associating with pY120 and pY129 peptides by MS, we identified new interactions between M2 and PLCγ2, p85α, adaptor protein NCK1, and the SHP2 phosphatase. Each phosphomotif of M2 constitutes a specific, independent interaction region for the different full-length proteins. The $Tyr(P)^{120}$ motif interacted with Fyn, Lyn, Vav1, and NCK1; the $Tyr(P)^{129}$ motif associated with PLCγ2 and SHP2; and both phosphomotifs interacted equally with p85α. Direct association of the cellular proteins with the M2 phosphomotifs was mediated by SH2 domains. The binding affinities of the individual SH2 domains for each phosphomotif varied from ~100 nM (strong binding) to ~17 μM (weak binding), which is within the affinity range of 100 nM to 10 μM described for SH2-Tyr(P) interactions (35). Direct binding analyses revealed additional overlapping specificities, as is the case for the SH2 domains of Fyn, Lyn, Vav1, and NCK1 that bound both phosphomotifs despite having a greater affinity for pY120. Within the subset of proteins containing dual SH2 domains, our results indicate that the C-terminal SH2 domains of PLCγ2 and p85α and the N-terminal SH2 domain of SHP2 mediate direct association of the full-length proteins with M2 phosphosites. Given that PLCγ2 associated abundantly and exclusively with pY129, we were surprised that its C-terminal SH2 domain bound tightly to both phosphopeptides. It is possible that association of PLCγ2 with pY129 was enhanced by indirect interactions or that, in the context of the full-length protein, the affinity of its C-terminal SH2 domain for pY129 is higher than that of the isolated domain. Consistent with this idea, other results have shown that Vav1 and PLCγ family members interact physically and functionally in lymphoid cells (36). All other binding affinities correlated with the specificity of the full-length proteins for M2 phosphopeptides.

M2 expression drove robust tyrosine phosphorylation of PLCγ2 in B cells. By analogy to the M2-Fyn-Vav1 complex that drives Vav1 phosphorylation, M2 may also act as an adaptor toward PLCγ2, bringing it into the vicinity of an Src family kinase and promoting its phosphorylation. Corroborating this idea is the fact that Fyn co-immunoprecipitates with PLCγ2 and M2. Both M2 phosphomotifs were required to induce phosphorylation of PLCγ2, suggesting that the $Tyr(P)^{129}$ motif, despite having lower levels of phosphorylation than the $Tyr(P)^{120}$ motif (5), works as an effective SH2 docking site. The pattern of M2-driven PLCγ2 tyrosine phosphorylation is similar to that induced by BCR stimulation and indicates that M2 is activating the PLCγ2 pathway, but this needs further confirmation. Similarly, K1 also induces constitutive tyrosine phosphorylation of PLCγ2. Although the phosphorylation sites have not been identified, K1 was shown to activate the PLCγ2 pathway (3, 37). The C-terminal Tyr residues of PLCγ2 appeared to have a higher contribution to the total phosphorylation of the protein upon M2 expression. Phosphorylation of Tyr^{753} and Tyr^{759} predominantly depends on Btk/Tec kinases and correlates with the catalytic activation of PLCγ2 (23, 24, 26, 38). Phosphorylation of Tyr^{1197} and Tyr^{1217} is largely Btk-independent and is likely to depend on Src family kinases, but its role in PLCγ2 signaling is unclear (23, 25, 26). The close association of M2 with Src family kinases may favor phosphorylation on these C-terminal residues.

Surprisingly, M2 expression had an inhibitory effect on AKT. This suggests that M2 may inhibit PI3K activity and contrasts with the effect of K1, LMP1, and LMP2A, which activate the PI3K/AKT pathway (39–41). Thus, it is possible that the inhibitory effect exerted on PI3K by M2 may be compensated by selective activation of PLCγ2 and Vav1. Similar to M2, p85α contains a proline-rich peptide that binds the SH3 domains of Fyn and Lyn. This interaction leads to increased catalytic activity of the PI3K (42). The inhibitory effect of M2 could be simply due to competition, by preventing the SH3 domains of those Src family tyrosine kinases from binding p85α and activating PI3K. However, the M2 double tyrosine to phenylalanine mutant protein failed to inhibit AKT activation, indicating that M2 phosphorylation is required for this effect (Fig. 5, *A–C*). Another possible mechanism for the M2 inhibition of AKT would be the sequestration of the p85α by M2 through Tyr(P)-SH2 interactions, which could prevent activation of PI3K.

The C-terminal PRR of M2 has several roles in M2 signaling. First, it mediates robust association with Vav1, a main target of M2 in several ectopic expression systems (5, 6). Second, it is required for tyrosine phosphorylation of M2 to create additional docking sites on the protein. Here, this region of M2 is shown to bind directly and strongly, within the known affinity range of SH3 domains for proline-rich regions (43), to the SH3 domains of Fyn and Lyn. Both this C-terminal PRR and Src family kinase expression are required to concentrate M2 near the plasma membrane. These results support a model in which direct association of M2 with Src family kinases via a C-terminal PRR-SH3 interaction would recruit M2 to the plasma membrane and lead to its phosphorylation. The predominance of M2 at the plasma membrane in B cells could be due to the presence of specific Src family kinases. Because M2 localization

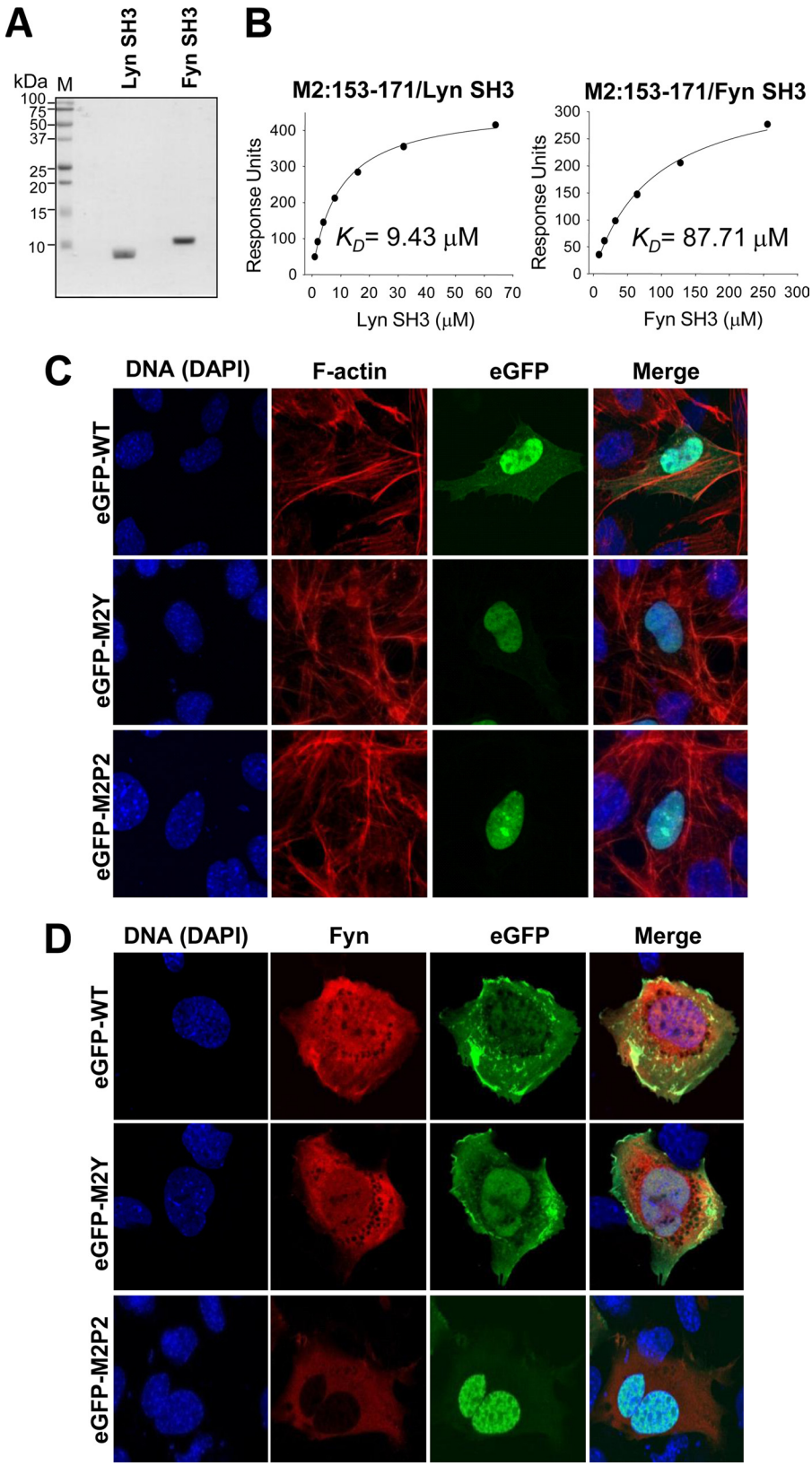

FIGURE 7. **Localization of M2 to membrane ruffles is dependent on the expression of Src family tyrosine kinases.** *A*, Coomassie Blue-stained SDS-polyacrylamide gel depicting the purified SH3 domains used in SPR experiments. *M*, molecular weight markers. *B*, the C-terminal PRR of M2 binds directly to the SH3 domains of Lyn and Fyn with distinct affinities. The SH3 domains of Fyn and Lyn were injected at a range of concentrations, at 10 μl/min, over immobilized M2(153–171) peptide (~140 RU) or an empty control cell. Equilibrium binding values were plotted against analyte concentration, and the K_D value was determined by non-linear fitting of the data. Data are representative of two independent experiments. *C*, localization of eGFP-tagged wild type M2, M2Y, and M2P2 proteins transiently expressed in SYF cells. F-actin was detected with TRITC-phalloidin. *D*, SYF cells ectopically expressing HA-tagged Fyn and eGFP-M2 proteins. Fyn was detected with an anti-HA primary antibody followed by staining with an Alexa Fluor 594-conjugated secondary antibody.

in B cells is independent of Src family kinase activity, it is likely that the kinase is directly recruiting M2 rather than indirectly affecting M2 localization through phosphorylation of a bridge protein or modulation of the actin cytoskeleton. Upon tyrosine phosphorylation, M2 forms a wider range of complexes, a process that is probably regulated by the level of M2 phosphorylation, the local concentration and conformation of the cellular partners, and the affinity of their SH2 and SH3 domains for M2.

The M2 sequence encompassing Tyr^{120} and Tyr^{129} does not form a consensus ITAM (Fig. 1*A*). However, there are similarities, such as the close proximity between the tyrosine residues and similar sequence identity of the Tyr^{129} motif (Y^{129}IQP) to the second motif of the K1 ITAM (YTQP) (44). We propose that M2 encoded by MuHV-4, like LMP1, LMP2A, K1, and K15, modulates B cell signaling, but contrary to the latter proteins, it is a soluble cytoplasmic protein with a juxtamembranar localization that recruits SH2-containing cellular proteins through an unconventional ITAM.

Acknowledgment—We thank António Temudo for help with confocal microscopy.

REFERENCES

1. Damania, B. (2004) Oncogenic γ-herpesviruses. Comparison of viral proteins involved in tumorigenesis. *Nat. Rev. Microbiol.* **2,** 656–668
2. Dal Porto, J. M., Gauld, S. B., Merrell, K. T., Mills, D., Pugh-Bernard, A. E., and Cambier, J. (2004) B cell antigen receptor signaling 101. *Mol. Immunol.* **41,** 599–613
3. Lee, B. S., Lee, S. H., Feng, P., Chang, H., Cho, N. H., and Jung, J. U. (2005) Characterization of the Kaposi's sarcoma-associated herpesvirus K1 signalosome. *J. Virol.* **79,** 12173–12184
4. Virgin, H. W., 4th, Latreille, P., Wamsley, P., Hallsworth, K., Weck, K. E., Dal Canto, A. J., and Speck, S. H. (1997) Complete sequence and genomic analysis of murine γ-herpesvirus 68. *J. Virol.* **71,** 5894–5904
5. Pires de Miranda, M., Alenquer, M., Marques, S., Rodrigues, L., Lopes, F., Bustelo, X. R., and Simas, J. P. (2008) The γ-herpesvirus m2 protein manipulates the Fyn/Vav pathway through a multidocking mechanism of assembly. *PLoS One* **3,** e1654
6. Rodrigues, L., Pires de Miranda, M., Caloca, M. J., Bustelo, X. R., and Simas, J. P. (2006) Activation of Vav by the γ-herpesvirus M2 protein contributes to the establishment of viral latency in B lymphocytes. *J. Virol.* **80,** 6123–6135
7. Siegel, A. M., Herskowitz, J. H., and Speck, S. H. (2008) The MHV68 M2 protein drives IL-10 dependent B cell proliferation and differentiation. *PLoS Pathog.* **4,** e1000039
8. Jacoby, M. A., Virgin, H. W. 4th, and Speck, S. H. (2002) Disruption of the M2 gene of murine γ-herpesvirus 68 alters splenic latency following intranasal, but not intraperitoneal, inoculation. *J. Virol.* **76,** 1790–1801
9. Macrae, A. I., Usherwood, E. J., Husain, S. M., Flaño, E., Kim, I. J., Woodland, D. L., Nash, A. A., Blackman, M. A., Sample, J. T., and Stewart, J. P. (2003) Murid herpesvirus 4 strain 68 M2 protein is a B-cell-associated antigen important for latency but not lymphocytosis. *J. Virol.* **77,** 9700–9709
10. Simas, J. P., Marques, S., Bridgeman, A., Efstathiou, S., and Adler, H. (2004) The M2 gene product of murine γ-herpesvirus 68 is required for efficient colonization of splenic follicles but is not necessary for expansion of latently infected germinal centre B cells. *J. Gen. Virol.* **85,** 2789–2797
11. Liang, X., Shin, Y. C., Means, R. E., and Jung, J. U. (2004) Inhibition of interferon-mediated antiviral activity by murine γ-herpesvirus 68 latency-associated M2 protein. *J. Virol.* **78,** 12416–12427
12. Herskowitz, J. H., Siegel, A. M., Jacoby, M. A., and Speck, S. H. (2008) Systematic mutagenesis of the murine γ-herpesvirus 68 M2 protein identifies domains important for chronic infection. *J. Virol.* **82,** 3295–3310
13. Songyang, Z., Shoelson, S. E., McGlade, J., Olivier, P., Pawson, T., Bustelo, X. R., Barbacid, M., Sabe, H., Hanafusa, H., and Yi, T. (1994) Specific motifs recognized by the SH2 domains of Csk, 3BP2, fps/fes, GRB-2, HCP, SHC, Syk, and Vav. *Mol. Cell Biol.* **14,** 2777–2785
14. Scheich, C., Kümmel, D., Soumailakakis, D., Heinemann, U., and Büssow, K. (2007) Vectors for co-expression of an unrestricted number of proteins. *Nucleic Acids Res.* **35,** e43
15. Shevchenko, A., Wilm, M., Vorm, O., and Mann, M. (1996) Mass spectrometric sequencing of proteins silver-stained polyacrylamide gels. *Anal. Chem.* **68,** 850–858
16. Perkins, D. N., Pappin, D. J., Creasy, D. M., and Cottrell, J. S. (1999) Probability-based protein identification by searching sequence databases using mass spectrometry data. *Electrophoresis* **20,** 3551–3567
17. López-Lago, M., Lee, H., Cruz, C., Movilla, N., and Bustelo, X. R. (2000) Tyrosine phosphorylation mediates both activation and downmodulation of the biological activity of Vav. *Mol. Cell Biol.* **20,** 1678–1691
18. Rodrigues, L., Filipe, J., Seldon, M. P., Fonseca, L., Anrather, J., Soares, M. P., and Simas, J. P. (2009) Termination of NF-κB activity through a γ-herpesvirus protein that assembles an EC5S ubiquitin-ligase. *EMBO J.* **28,** 1283–1295
19. Klinghoffer, R. A., Sachsenmaier, C., Cooper, J. A., and Soriano, P. (1999) Src family kinases are required for integrin but not PDGFR signal transduction. *EMBO J.* **18,** 2459–2471
20. Bustelo, X. R. (2000) Regulatory and signaling properties of the Vav family. *Mol. Cell Biol.* **20,** 1461–1477
21. Bustelo, X. R., Rubin, S. D., Suen, K. L., Carrasco, D., and Barbacid, M. (1993) Developmental expression of the vav protooncogene. *Cell Growth Differ.* **4,** 297–308
22. Usherwood, E. J., Stewart, J. P., and Nash, A. A. (1996) Characterization of tumor cell lines derived from murine γ-herpesvirus-68-infected mice. *J. Virol.* **70,** 6516–6518
23. Humphries, L. A., Dangelmaier, C., Sommer, K., Kipp, K., Kato, R. M., Griffith, N., Bakman, I., Turk, C. W., Daniel, J. L., and Rawlings, D. J. (2004) Tec kinases mediate sustained calcium influx via site-specific tyrosine phosphorylation of the phospholipase Cγ Src homology 2-Src homology 3 linker. *J. Biol. Chem.* **279,** 37651–37661
24. Kim, Y. J., Sekiya, F., Poulin, B., Bae, Y. S., and Rhee, S. G. (2004) Mechanism of B-cell receptor-induced phosphorylation and activation of phospholipase C-γ2. *Mol. Cell Biol.* **24,** 9986–9999
25. Ozdener, F., Dangelmaier, C., Ashby, B., Kunapuli, S. P., and Daniel, J. L. (2002) Activation of phospholipase Cγ2 by tyrosine phosphorylation. *Mol. Pharmacol.* **62,** 672–679
26. Rodriguez, R., Matsuda, M., Perisic, O., Bravo, J., Paul, A., Jones, N. P., Light, Y., Swann, K., Williams, R. L., and Katan, M. (2001) Tyrosine residues in phospholipase Cγ 2 essential for the enzyme function in B-cell signaling. *J. Biol. Chem.* **276,** 47982–47992
27. Watanabe, D., Hashimoto, S., Ishiai, M., Matsushita, M., Baba, Y., Kishimoto, T., Kurosaki, T., and Tsukada, S. (2001) Four tyrosine residues in phospholipase C-γ2, identified as Btk-dependent phosphorylation sites, are required for B cell antigen receptor-coupled calcium signaling. *J. Biol. Chem.* **276,** 38595–38601
28. Bunney, T. D., and Katan, M. (2011) PLC regulation. Emerging pictures for molecular mechanisms. *Trends Biochem. Sci.* **36,** 88–96
29. Andjelković, M., Alessi, D. R., Meier, R., Fernandez, A., Lamb, N. J., Frech, M., Cron, P., Cohen, P., Lucocq, J. M., and Hemmings, B. A. (1997) Role of translocation in the activation and function of protein kinase B. *J. Biol. Chem.* **272,** 31515–31524
30. Alessi, D. R., Andjelkovic, M., Caudwell, B., Cron, P., Morrice, N., Cohen, P., and Hemmings, B. A. (1996) Mechanism of activation of protein kinase B by insulin and IGF-1. *EMBO J.* **15,** 6541–6551
31. Albrecht, J. C., Friedrich, U., Kardinal, C., Koehn, J., Fleckenstein, B., Feller, S. M., and Biesinger, B. (1999) Herpesvirus ateles gene product Tio interacts with nonreceptor protein tyrosine kinases. *J. Virol.* **73,** 4631–4639
32. Pietrek, M., Brinkmann, M. M., Glowacka, I., Enlund, A., Hävemeier, A., Dittrich-Breiholz, O., Kracht, M., Lewitzky, M., Saksela, K., Feller, S. M., and Schulz, T. F. (2010) Role of the Kaposi's sarcoma-associated herpesvirus K15 SH3 binding site in inflammatory signaling and B-cell activation.

J. Virol. **84,** 8231–8240
33. Schweimer, K., Hoffmann, S., Bauer, F., Friedrich, U., Kardinal, C., Feller, S. M., Biesinger, B., and Sticht, H. (2002) Structural investigation of the binding of a herpesviral protein to the SH3 domain of tyrosine kinase Lck. *Biochemistry* **41,** 5120–5130
34. Sandilands, E., Brunton, V. G., and Frame, M. C. (2007) The membrane targeting and spatial activation of Src, Yes and Fyn is influenced by palmitoylation and distinct RhoB/RhoD endosome requirements. *J. Cell Sci.* **120,** 2555–2564
35. Ladbury, J. E., Lemmon, M. A., Zhou, M., Green, J., Botfield, M. C., and Schlessinger, J. (1995) Measurement of the binding of tyrosyl phosphopeptides to SH2 domains. A reappraisal. *Proc. Natl. Acad. Sci. U.S.A.* **92,** 3199–3203
36. Caloca, M. J., Zugaza, J. L., and Bustelo, X. R. (2008) Mechanistic analysis of the amplification and diversification events induced by Vav proteins in B-lymphocytes. *J. Biol. Chem.* **283,** 36454–36464
37. Lagunoff, M., Majeti, R., Weiss, A., and Ganem, D. (1999) Deregulated signal transduction by the K1 gene product of Kaposi's sarcoma-associated herpesvirus. *Proc. Natl. Acad. Sci. U.S.A.* **96,** 5704–5709
38. Gresset, A., Hicks, S. N., Harden, T. K., and Sondek, J. (2010) Mechanism of phosphorylation-induced activation of phospholipase C-γ isozymes. *J. Biol. Chem.* **285,** 35836–35847
39. Dawson, C. W., Tramountanis, G., Eliopoulos, A. G., and Young, L. S. (2003) Epstein-Barr virus latent membrane protein 1 (LMP1) activates the phosphatidylinositol 3-kinase/Akt pathway to promote cell survival and induce actin filament remodeling. *J. Biol. Chem.* **278,** 3694–3704
40. Swart, R., Ruf, I. K., Sample, J., and Longnecker, R. (2000) Latent membrane protein 2A-mediated effects on the phosphatidylinositol 3-kinase/Akt pathway. *J. Virol.* **74,** 10838–10845
41. Tomlinson, C. C., and Damania, B. (2004) The K1 protein of Kaposi's sarcoma-associated herpesvirus activates the Akt signaling pathway. *J. Virol.* **78,** 1918–1927
42. Pleiman, C. M., Abrams, C., Gauen, L. T., Bedzyk, W., Jongstra, J., Shaw, A. S., and Cambier, J. C. (1994) Distinct p53/56lyn and p59fyn domains associate with nonphosphorylated and phosphorylated Ig-α. *Proc. Natl. Acad. Sci. U.S.A.* **91,** 4268–4272
43. Li, S. S. (2005) Specificity and versatility of SH3 and other proline-recognition domains. Structural basis and implications for cellular signal transduction. *Biochem. J.* **390,** 641–653
44. Lee, H., Guo, J., Li, M., Choi, J. K., DeMaria, M., Rosenzweig, M., and Jung, J. U. (1998) Identification of an immunoreceptor tyrosine-based activation motif of K1 transforming protein of Kaposi's sarcoma-associated herpesvirus. *Mol. Cell Biol.* **18,** 5219–5228

Role of Src Homology Domain Binding in Signaling Complexes Assembled by the Murid γ-Herpesvirus M2 Protein

Marta Pires de Miranda, Filipa B. Lopes, Colin E. McVey, Xosé R. Bustelo and J. Pedro Simas

J. Biol. Chem. 2013, 288:3858-3870.
doi: 10.1074/jbc.M112.439810 originally published online December 20, 2012